Bioresource Technology 438 (2025) 133262

Contents lists available at ScienceDirect

Bioresource Technology

journal homepage: www.elsevier.com/locate/biortech

Chlorella vulgaris heterotrophy-to-phototrophy conversion dynamics are mostly independent of light intensity

Wendie Levasseur [1], Victor Pozzobon [*,1]

Université Paris-Saclay, CentraleSupélec, Laboratoire de Génie des Procédés et Matériaux, Centre Européen de Biotechnologie et de Bioéconomie (CEBB), 3 rue des Rouges Terres, 51110 Pomacle, France

HIGHLIGHTS

- *Chlorella vulgaris* transition from heterotrophy to phototrophy was studied.
- Five stages were identified including PSU repair, pigment expression, cell division.
- Characteristic times were identified for each mechanism.
- The process appears to be mostly independent of the applied light intensity.
- Inoculum physiological state has only a marginal effect.

GRAPHICAL ABSTRACT

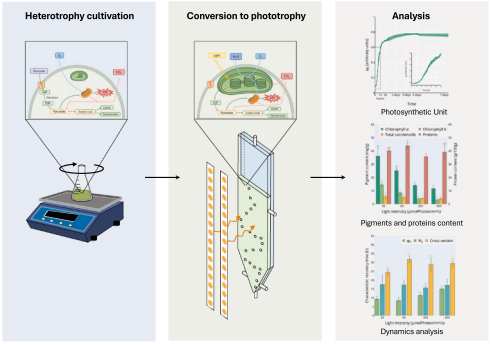

ARTICLE INFO

Keywords:
Microalgae
Trophic conversion
Metabolism
Photosystem II
Pigment
Protein

ABSTRACT

Trophic conversion – a sequential cultivation strategy combining heterotrophic and phototrophic growth – offers a promising route for large-scale microalgae production by coupling the high biomass yields of heterotrophy with the biochemical advantages of phototrophy. Despite its potential, the cellular mechanisms governing this transition remain poorly understood. Here is presented the first mechanistic dissection of trophic conversion in *Chlorella vulgaris*, using isoactinic light conditions (30–600 μmol photons/m^2/s) and inocula with varied physiological states. A consistent five-step cellular response was identified: initiation of gene expression, recovery of PhotoSystem II activity, reactivation of cell division, restoration of pigment biosynthesis, and establishment of steady-state growth, all culminating in full restoration of the phototrophic phenotype. These phases follow distinct timelines (3 h, 9–17 h, 24 h, 32 h, and 72 h, respectively) and exhibit specific light dependencies, as characterized in this study. These findings provide a mechanistic framework to guide the optimization of trophic conversion at the process level.

* Corresponding author.
E-mail address: victor.pozzobon@centralesupelec.fr (V. Pozzobon).
[1] Both author contributed equally to this work.

https://doi.org/10.1016/j.biortech.2025.133262
Received 16 July 2025; Received in revised form 27 August 2025; Accepted 1 September 2025
Available online 3 September 2025

1. Introduction

Microalgae – photosynthetic microorganisms found in fresh or marine water – are primarily recognized for their essential role in sustaining ecosystems. Notably, they generate approximately 50 % of the Earth's annual oxygen supply (Behrenfeld, 2001) and play a central role in oceanic biogeochemical cycles (Hutchins and Fu, 2017; Levine and Leles, 2021). Less widely known, however, is their emerging potential as a biotechnological platform for producing medium- to high-value biomolecules, ranging from food and feed additives (Madeira, 2017) to nutraceutical pigments (Camarena-Bernard and Pozzobon, 2024). Conceptually, cultivating photosynthetic microalgae on a large scale presents a triple-win opportunity. Environmentally, it offers a pathway to reduce the footprint of target molecules while providing additional benefits such as carbon cycling and mitigation of nitrate and phosphorus pollutions (Posadas et al., 2015). Socially, it holds the promise of creating high-quality employment: for instance, the biomolecule bioeconomy (encompassing chemicals, pharmaceuticals, and biofuels) generates €139 000 in added value per worker annually – significantly more than the €22 000 per worker per year in traditional agricultural bioeconomy (Ronzon et al., 2022) –. Despite these promises, photoautotrophic microalgae have struggled to expand beyond their historical cradles: aquaculture and food, in some niche markets such as Japan.

Indeed, large-scale cultivation is where the strength of microalgae becomes their weakness. In contrast to the ocean, where they are present in dilute quantities, microalgae are driven to very high concentrations in industrial systems (1–10 g/L (Ruiz, 2016). As a result, incoming light is entirely absorbed within the first few millimeters of the culture vessel, leaving the bulk of the culture in the dark. This part of the culture is said to be in an aphotic state where little to no photosynthesis occurs, and in some cases, respiration dominates, leading to net biomass loss. Options to remediate this problem are few and far from ideal. One strategy involves increasing the surface-to-volume ratio of the system to enhance light capture and reduce the depth of the aphotic zone (Qiang et al., 1998; Pulz, 2001). However, this comes at the cost of significantly higher capital expenditure. Alternatively, more light could be supplied via LEDs. This avenue would increase the energy demand and void environmental benefits of the cultivation process (Oliver et al., 2023). Finally, one could genetically engineer microalgae to reduce their light harvesting capacity, thus allowing deeper light penetration. This raises concerns around the deployment of genetically modified microorganisms (GMMs) at scale and has not yet been conclusive from a technical point of view (de Mooij et al., 2016).

Acknowledging the biotechnological potential of microalgae and the barrier that is photosynthesis, some authors came up with the idea of resorting to heterotrophy to massively produce microalgae. Indeed, heterotrophic cultivation bypasses photosynthesis constraints by allowing light-independent cell production. While it is difficult to estimate the number of heterotrophy-capable strains, about half of the microalgae with biotechnological potential could rely solely on an organic carbon source (glucose or acetate, most of the time) to support their proliferation (Gladue and Maxey, 1994). Strains capable of such metabolic flexibility tend to proliferate faster and reach higher final concentrations compared to their photosynthetic counterparts. Furthermore, from a biotechnological perspective, relying on this mode of production allows taking advantage of brewery millennial know-how and techno-economical ecosystem (efficient culture protocols, robust supply chain, affordable installations), another major advantage.

Still, as always, there is no free lunch. Relying on heterotrophy voids most of the environmental benefits associated with photosynthetic cultivation. Moreover, microalgae grown heterotrophically tend to be of lower biochemical quality, typically exhibiting reduced protein and pigment content (Barros, 2019). Facing this dilemma, scholars and engineers came up with the idea of chaining the heterotrophy and phototrophy, with the hope of getting the best of each one, in a sequential manner. This idea led to a strain of research on this strategy, with a particular focus on pigment production.

The first proof of concept was introduced by Ogbonna et al. (1997) in the late 1990s. However, it is only a decade later that the strategy emerged again as Sequential Heterotrophy-Dilution-Photoinduction (Fan, 2012), and progressively optimized for biomass and pigment production (Kim, 2020), with astaxanthin (Wan, 2015) and lutein (Zhang, 2025; Chen, 2022) as targets.

It is also around that time that the wastewater treatment community investigated the strategy in an unrelated fashion. For these researchers, the idea was twofold. First, they showed that the phenotypic transition drove the cells to uptake higher quantities of nitrogen and phosphorus from wastewaters (Wang et al., 2015). Second, they leveraged the higher initial cell density to shorten the bioremediation process duration and make it more resilient to bacterial competition (Zhou, 2012; Zheng et al., 2012). Some teams went even further and maximized the process efficiency by nitrogen-starving the heterotrophic cells in order to trigger luxury intake (cells absorbing more than what they need in order to build up some stocks to face another potential starvation) (Brown and Shilton, 2014; Xie et al., 2017; Masojídek, 2021).

Despite the aforementioned efforts, much remains to be done. Indeed, most studies have approached the topic from a bioprocess perspective. They relied on trial-and-error strategies and empirical observations. While these efforts have yielded some practical outcomes, they delivered limited insight into the biological mechanisms at play. This is all the more unfortunate as the few studies that have associated some hints of biological-related methodologies tend to show that there is more to be found. For example, the photosynthetic apparatus seems to recover its functionality within 24–48 h (Babaei, 2020; Levasseur et al., 2023), while pigment expression seems to take a longer time. Still, while this observation calls for hour-resolved process monitoring, one or two samples a day is still the conventional way to go in this field. Furthermore, the absence of a unified terminology also reflects the nascent and fragmented nature of this field where multiple denominations compete (trophic conversion, metabolic shift, concentration-shift method, sequential heterotrophy-dilution-photoinduction, sequential heterotrophic/autotrophic cultivation, two-stage strategy, …) showing no consensus to date.

This article takes up the torch and moves beyond procedural optimization to address the underlined knowledge gap. It focuses on the photosynthetic recovery dynamics at an hourly resolution and casts for the first time light into cell-level mechanisms at play during a trophic conversion. By bringing unprecedented knowledge, the article hopes to help scholars and engineers better elaborate their trophic conversion processes.

2. Materials and methods

2.1. Microalgae strain, growth medium, and seed culture

Chlorella vulgaris SAG 211-11b was obtained from the Culture Collection of Algae at Göttingen University (SAG), Germany. The strain was originally maintained under phototrophic conditions using B3N medium (See Supplementary Materials) (Shibata, 1959). Still, before starting the trophic conversion experiments, it was subcultured under heterotrophic conditions for more than two consecutive months. Heterotrophic subculturing was carried out using a modified B3N medium, prepared at twice its standard concentration (2xB3N) and Supplemented with 20 g/L of glucose (See Supplementary Materials). Cultures were grown in the absence of light, at 25 °C, without CO_2 supply, and under constant agitation at 100 rpm in 50 mL of culture medium in 250 mL flasks. The heterotrophic cultures were subcultured regularly, ensuring a fixed interval of 11 days between the last subculturing and the start of the experiments.

2.2. Trophic conversion process

The trophic conversion process starts by harvesting an 11-day-old heterotrophic subculture and dividing it into two. The first part is used to perform all the start point analyses, including biomass density to standardize starting point concentration. The second part was taken as an aliquot and standardized at a density of 0.2 g/L (dilution in glucose-free B3N medium, ensuring residual glucose concentration below 0.2 g/L) before being injected into the ultrathin flat panel photobioreactors (Fig. 1).

The ultrathin flat panel photobioreactors were designed to ensure homogeneous illumination within their volume. To achieve this, they feature both a low-thickness culture compartment (6 mm) and an absorbed light monitoring system, triggering a dilution (with glucose-free B3N medium) as soon as exiting illumination falls below 80 % of the incident value (turbidostat mode of operation). Furthermore, low initial density inoculation ensures that all the runs unfold under a homogeneous illumination. In terms of technical details, the ultrathin photobioreactors feature a 125-mL working volume, are sparged with air enriched with 2.5 % CO_2 (flow rate of 1.8 Vessel Volume per Minute), and have a compartment dedicated to temperature control (25 °C, maintenance by water circulation). The main drawback of this system is that, overall, it harbors little biomass, making cell characterization throughout only possible upon harvesting the whole culture volume (after 7 days of culture, referred to as end point analysis).

2.3. Sampling frequency & performed analyses

The experiments were conducted in biological triplicate, with three photobioreactors running in parallel to assess reproducibility. Samples (3 mL) were collected from each reactor every hour for the first 12 h, then every two hours up to 30 h, and subsequently twice per day until the end of the experiment, which lasted 7 days. Each assay describes a physiological function associated with photosynthesis and spans over a specific biological level (photosynthetic units, individual cell, or population). They can be listed from the most precise ones to the broadest ones. First comes the PhotoSystem II (PSII) quantum yield (*i.e.*, its ability to channel light energy to the special pair of chlorophyll *a* molecules, φ_0), PSII ability to recover an electron using the conveyed light energy (Ψ_0), general functioning of the photosynthetic apparatus, cell optical cross section (*i.e.*, light absorption over the visible spectrum used as proxy of the cell total pigment content), cell size (to identify division patterns), and population viability.

In addition, to quantify the response amplitude, biomass was fully characterized at both the start and end points. This included measurements of protein and pigment content, as well as an assessment of the photosynthetic apparatus, providing a reference point to evaluate the extent of recovery under different light treatments. Intermediate time points were used to capture the dynamics of photosynthetic activity restoration by regularly monitoring the functional state of the photosynthetic apparatus. In conjunction, cell absorption cross section (a proxy of cell pigment content) was measured using opal glass transmission method (Moheimani et al., 2013). Additionally, cells viability, size, and complexity (probed using light redirected sideways by organelles, starch granules, etc.), and chlorophyll autofluorescence were tracked using flow cytometry, offering detailed insight into the physiological changes occurring throughout the transition Finally, optical density was also monitored externally, even though regulated by the ultrathin flat panel photobioreactors, as a safeguard procedure.

2.4. Photosynthetic apparatus qualification

Upon withdrawing from the photobioreactor, fresh samples were placed in a dark chamber for 15 min to allow for dark acclimation.

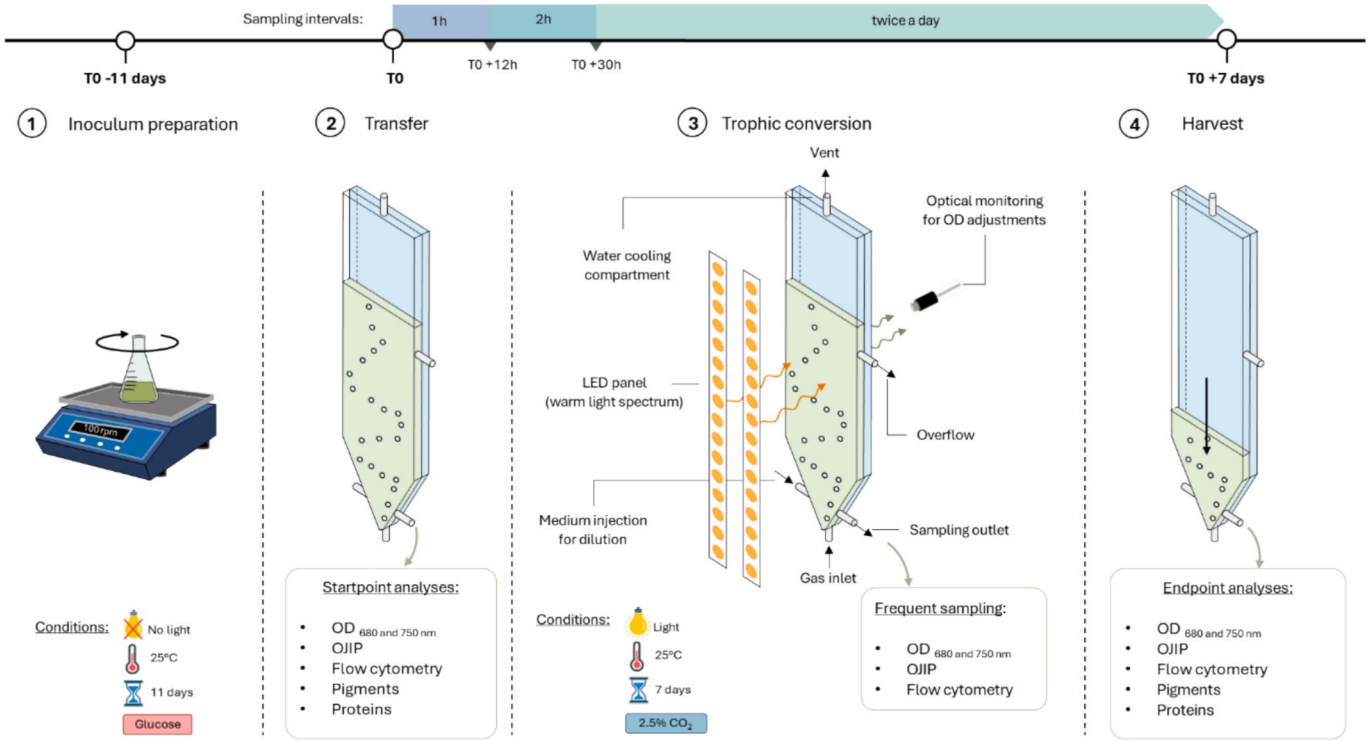

Fig. 1. Schematic of the trophic conversion process experiments. 1. Inoculation preparation, by subculturing of an aliquot from a mother culture acclimated for more than two months to heterotrophy. 2. Transfer to an ultrathin flat panel photobioreactor containing glucose-free B3N medium. 3. Cultivation phase (turbidostat mode of operation) with time-dependent sampling pattern (every hour at the beginning, to twice a day at the end, sampling volume: 3 mL). 4. Harvest of the culture (7 days after inoculation). Experiments were triplicated simultaneously using three exact replicates, placed in the same enclosure to avoid external light perturbation and ensure common surrounding conditions.

Following this acclimation period, an OJIP (a.k.a. fast fluorescence) assay was performed to assess the induction kinetics of chlorophyll *a* fluorescence, providing key information on the functionality of photosystem II (PSII) and the overall photosynthetic performance of the cells (*Fluorometer FL 6000 – PSI*). The data were analyzed following the recommendations of Strasser (Blanc, 2010).

First, the overall polyphasic fluorescence signal dynamics were examined by analyzing the succession of OJIP phases. The expected sequence is initial charge separation, followed by the reduction of the plastoquinone pool, ending with saturation. Then, the analysis focused on the functional state of the PSII, assessing two key parameters:

- energy transfer from the antennae to the reaction center, φ_0
- the ability to use the channel energy to recover an electron, Ψ_0

DCMU (3-(3,4-dichlorophenyl)-1,1-dimethylurea, 25 μM final concentration) tests were also performed to assess the potential involvement of the PQ pool in the unexpected behavior observed for long-term heterotrophically cultivated cells.

2.5. Flow cytometry assays

Flow cytometry was employed to track changes in cell size, morphological complexity, and chlorophyll autofluorescence over time, as well as to assess cell viability using a dual-staining (Propidium Iodide – PI –/Fluoresceine DiAcetate – FDA –) method. Measurements were conducted using a BD LSR Fortessa X-20 flow cytometer, equipped with five lasers: UV (355 nm), violet (405 nm), blue (488 nm), yellow-green (561 nm), and red (640 nm).

For unstained *Chlorella vulgaris* cells, three intrinsic signals were recorded: Forward SCatter (FSC) as a proxy for cell size, Side SCatter (SSC) for cell complexity, and chlorophyll autofluorescence (blue laser, channel 695/40 nm). Additionally, cell viability was determined using fluorescein diacetate (blue laser, channel 530/30 nm) and propidium iodide (yellow-green laser, channel 610/20 nm). FDA identifies metabolically active cells based on intracellular esterase activity, while PI selectively stains non-viable cells (via DNA binding) with compromised membrane integrity.

The staining protocol was adapted from a previously described method (Ho, 2013). A stock solution of FDA (Sigma Chemicals F-7378) was prepared at 12 mM in DiMethyl SulfOxide (DMSO, Fisher Scientific, >99 %) and diluted to a final working concentration of 120 μM in Milli-Q water. The working solution was stored at −20 °C, protected from light. Similarly, a PI (Sigma Chemicals P-4170) working solution was prepared at 1.5 mM in Milli-Q water and stored at 4 °C in the dark.

For staining, a 200 μL aliquot of the culture was mixed with 800 μL of FDA and 10 μL of PI, followed by incubation in the dark for 2 min. Cells were analyzed immediately after incubation. Between each sample analysis, the flow cytometer was rinsed with a tube of Milli-Q water to prevent cross-contamination.

For each sample, 100,000 events were recorded. Cells were identified based on their chlorophyll autofluorescence, size, and complexity signals.

2.6. Determination of dry weight

Dry weight content was measured in triplicate only at the beginning of the experiment on heterotrophic cultures to determine the dilution factor required for achieving a final concentration of 0.2 g/L in the reactor prior to phototrophic induction. For this measurement, 1 mL of culture was vacuum-filtered using a vacuum flask connected to a pump and a pre-weighed, pre-dried MCE membrane filter (MF-Millipore, 0.22 μm pore diameter). The retained biomass was rinsed with Milli-Q water to remove residual salts from the culture medium, then dried at 105 °C until weight stabilization (Porra, 1990). The filter was subsequently reweighed using a high-precision analytical balance (± 0.1 mg, MS304S Mettler Toledo).

2.7. Pigment extraction and quantification

The pigment extraction process was performed at the beginning and end of the runs. Samples were harvested and washed twice with Milli-Q water by centrifugation (11,000 rpm, 4 °C, 10 min). The biomass was then frozen (−20 °C) and freeze-dried for 24 h under primary desiccation using a freeze dryer (*Christ Alpha 1–2 LD+*).

For extraction, 2–4 mg of the resulting powder was homogenized in 5 mL of pure methanol using an MP Biomedicals FastPrep-42 bead beater. The mixture was then incubated in a water bath at 60 °C for 20 min to ensure complete pigment extraction, considering the known recalcitrance of *Chlorella vulgaris* (Wellburn, 1994). The supernatant was filtered through 0.22 μm filters before spectrophotometric analysis (*Shimadzu UV-1800 UV/Vis, dual beam*) in quartz cuvettes. Throughout the entire protocol, samples were protected from light to prevent pigment degradation.

Full absorbance spectra from 350 to 800 nm were recorded, and pigment concentrations (mg/L) were calculated based on Welburn's equations (Lichtenthaler and Buschmann, 2001) with Lichtenthaler's processing guidelines (Seabold and Perktold, 2010):

$$[\text{Chlorophyll a}](\text{mg/L}) = 16.72 \times A_{665.2\text{nm}} - 9.16 \times A_{652.4\text{nm}} \quad (1)$$

$$[\text{Chlorophyll b}](\text{mg/L}) = 34.09 \times A_{652.4\text{nm}} - 15.28 \times A_{665.2\text{nm}} \quad (2)$$

$$[\text{Total carotenoid}]\ (\text{mg/L}) = (1000 \times A_{470\text{nm}} - 1.63 \times [\text{Chlorophylla}] - 104.96 \times [\text{Chlorophyllb}])/221 \quad (3)$$

2.8. Protein quantification

Using the same washed and freeze-dried biomass, approximately 2 mg of sample was resuspended in 20 mL of Milli-Q water. Total nitrogen (TN) content was then analyzed using a TOC analyzer (*Shimadzu TOC-L*). Samples were thermally decomposed at 680 °C, producing nitrogen oxides (NOx), which were subsequently detected by chemiluminescence. A 1000 mg/L $NaNO_3$ solution, and several of its dilution (range 0.5 – 1000 mg/L), were used as the calibration standard. The total nitrogen concentration obtained (mg/L) was converted into protein content using a conversion factor of 4.57, as established by Lourenço *et al.* for microalgae (Sullivan and Feinn, 2012).

2.9. Statistical procedure & Data processing

Unless stated otherwise, data are presented as mean ± standard deviation of the three replicates. Statistical significance is assessed using ANOVA testing (two-tailed, post-hoc Honestly Significant Difference with Bonferroni correction, significance level $p < 0.05$) or Welch's (unpaired) *t*-test (for pairwise comparison, two-tailed, $p < 0.05$). The tests were performed using the *statsmodels* Python package (Barron, 2019).

Characteristic times were extracted from the time series using a dedicated fitting procedure. First of all, φ_0, Ψ_0, and cross-section signals were normalized for each run individually. Then, Barron's loss function was minimized using a Python algorithm [51] Eq. (4), with $c = 0.2$, and $\alpha = -4$). This loss function was chosen as it allows combining a quadratic fit with control of potentially outlying observations (*i.e.*, artifacts or abhorrent points do not over penalize the optimization procedure).

$$f(x, \alpha, c) = \frac{|\alpha - 2|}{\alpha}\left(\left(\frac{(x/c)^2}{|\alpha - 2|} + 1\right)^{\frac{\alpha}{2}} - 1\right) \quad (4)$$

First-order exponential rise modeling of normalized signals was led by integrating Equation (5), or Equation (6) for pseudo-first order

modeling. These equations can be used to fit any signal (*e.g.*, φ0 or Ψ0) featuring a monotonic rising trend reaching a plateau. The main parameter to be optimized is characteristic time τ.

$$\frac{dy}{dt} = \frac{1}{\tau}(1 - y) \text{for} t > t_{lag} \quad (5)$$

$$\frac{dy}{dt} = \frac{1}{\tau}\sqrt{1 - y} \text{for} t > t_{lag} \quad (6)$$

3. Results

First, *Chlorella vulgaris* cells were cultured using glucose for more than two months to ensure complete acclimation to heterotrophic culture condition. Then, an aliquot was inoculated in a specific ultra-thin flat panel photobioreactor, ensuring a tightly-controlled exposure to an illumination of 60 μmolPhoton/m^2/s (Fig. 1). This illumination level was chosen as it represents an *a priori* ideal condition, *i.e.*, 4 times the light intensity required for photosynthesis to surpass maintenance, but about 2 times lower than the saturation intensity (See Supplementary Materials) (Degen et al., 2001; Pozzobon, 2020).

Microalgae acclimation was monitored for 7 days, with high-frequency sampling over the first 24 h. Each assay describes a physiological function associated with photosynthesis which reacts, at their own pace, in a five-step photosynthesis recovery mechanism.

3.1. Step one: latent preparation

In the initial hours following re-exposure to light, all monitored indicators remained at consistently low and statistically stable levels (average p-value of 0.401, min. 0.078, max 0.885) (Fig. 2 A, insets). This is especially the case for the PSII-related measurements. The photosynthetic apparatus showed a non-functional state, characterized by a stable and high fluorescence signal over the OJIP test (Fig. 3 A&B). To confirm that this behavior was associated only with the PSII, DCMU-poisoned tests were carried out (Fig. 3 C&D). They showed no significant differences in signal ($p = 0.480$), reinforcing the conclusion that the stagnation was PSII-specific.

The duration of this initial lag differs for each indicator. The PSII-associated measurements stop stalling after 3 h (Ψ_0, φ_0, Fig. 2 A, insets). After this period, pigment cross section starts to show some hints of an increase (Fig. 2 A, insets). Yet, it is only after 8 h that it markedly takes off. Similarly, the population morphology does evolve notably until 8 to 12 h after light reintroduction (Fig. 2 B).

3.2. Step two: booting up photosynthetic units

The first noticeable change appears in the PSII's ability to channel light energy to the reaction center. Technically, it can be detected through the appearance of the initial inflection on the OJIP test reading (Fig. 3 A&B). Consequently, φ_0, the indicator associated with this very early stage of the photosynthetic process, rises from an initial value of 0.09 ± 0.00 to 0.77 ± 0.01 following a first-order exponential rise with a characteristic time of 8.4 ± 0.4 h (Fig. 2A).

Next comes the second PSII-related indicator, Ψ_0 (representing the efficiency of the light to electron energy conversion). Ψ_0 also exhibits a first-order trend, yet at a slower pace (characteristic time of 17.4 ± 0.9 h) and of different magnitude (from 0.02 ± 0.00 to 0.37 ± 0.01)

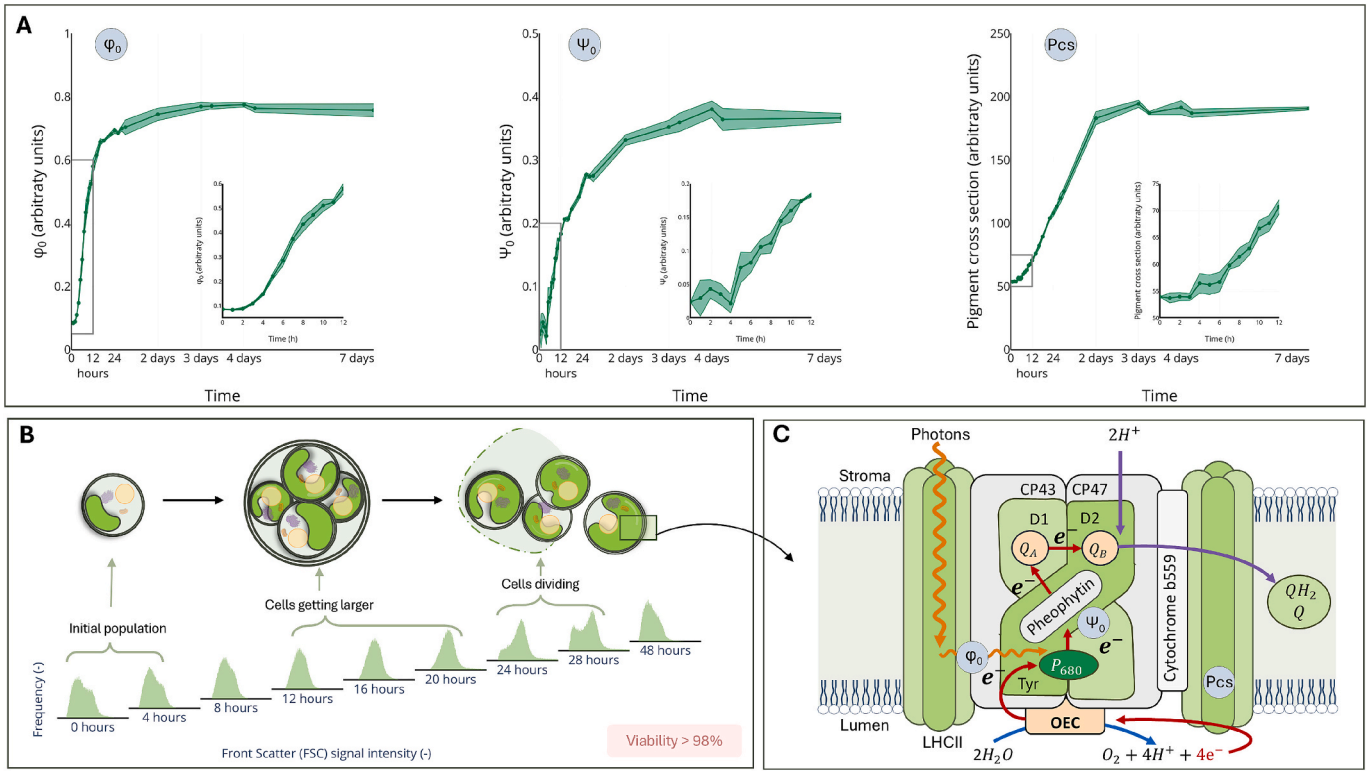

Fig. 2. Trophic conversion process of *Chlorella vulgaris* under 60 μmolPhoton/m^2/s (inoculum age: 11 days). A. Evolution over time of the indicators tied to the PSII status. φ_0 and Ψ_0 obtained via fast fluorescence induction assays (a.k.a. OJIP tests). Pigment cross-section measured using a diffuser-mounted spectrophotometer. Insets – Focus on the first 12 h. Solid line – mean of the three replicates. Shaded area – standard deviation (n = 3). Points – Measurements. B. General trend obtained by flow cytometry analysis. Histogram based on Front SCatter (FSC) signal (Blue laser 488 nm, 100 000 events) used as a proxy of cell size (zoomed on the first 48 h). Viability measured by Propidium Iodide/Fluoresceine DiAcetate dual staining, optimized for *Chlorella vulgaris* (Ho, 2013). The reported value is the minimum value encountered over the seven days for the three parallel runs. C. Schematic diagram of the functioning of the PhotoSystem II, with the key fluorometric indicators (φ_0 and Ψ_0) and pigment cross-section (Pcs) positioned. Orange arrow – Light. Red arrow – Electron flow. Blue arrow – Water splitting reaction. Purple arrows – Molecule (H^+ or plastoquinone) motion. Q – plastoquinone. QH_2 – plastoquinol.

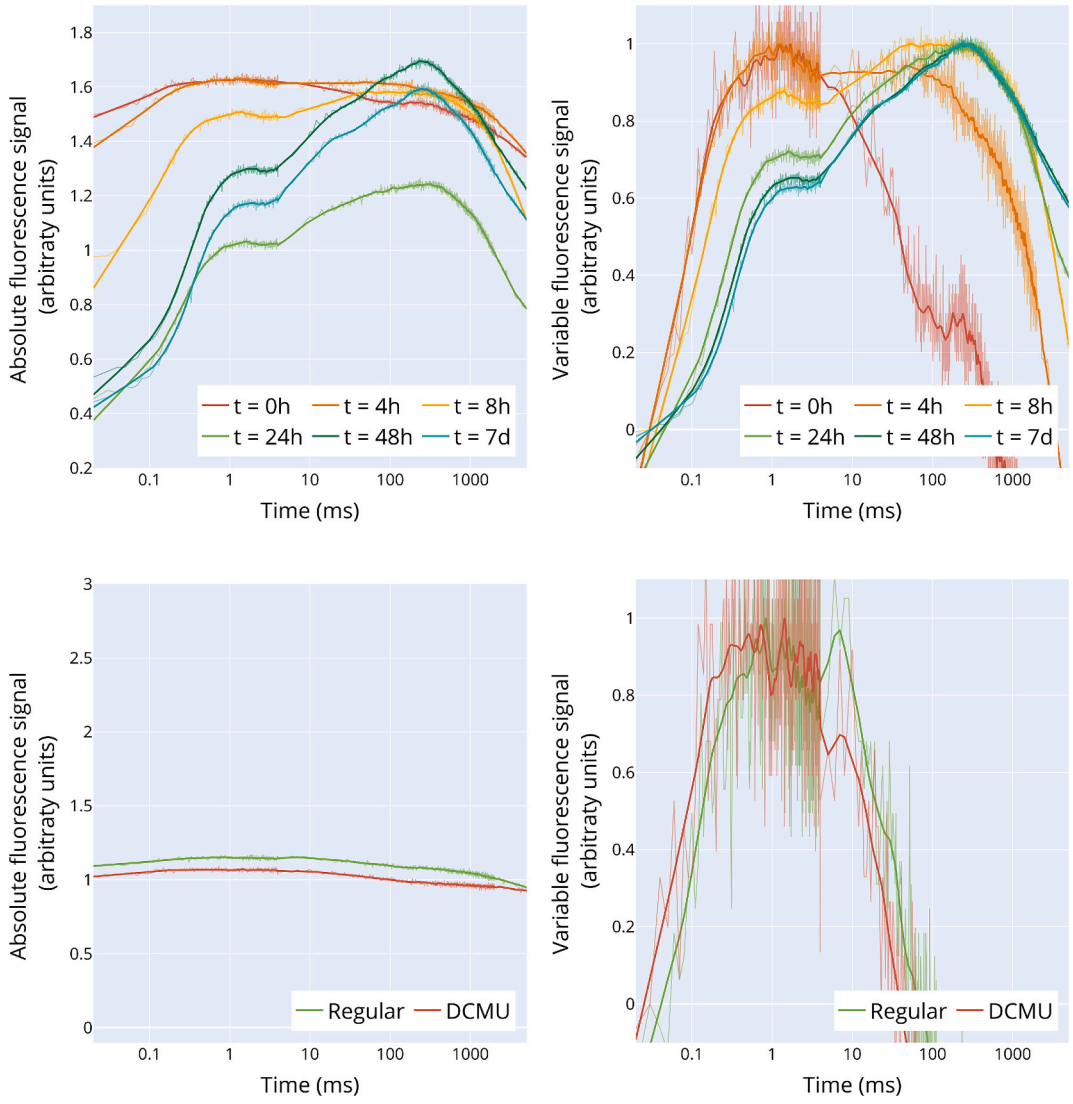

Fig. 3. Fast fluorescence induction assays (a.k.a. OJIP tests) readings. Saturating illumination of 3500 µmolPhoton/m2/s over 5 s. A. Raw (absolute) signal intensity for different samples drawn over the course of the trophic conversion process. B. Relative signal intensity for different samples drawn over the course of the trophic conversion process. Minimum fluorescent measurement after 50 µs following Strasser's guidelines \cite{strasser_fluorescence_2000}. Maximum fluorescence is taken as the curve's highest point. C Raw (absolute) signal intensity for start-point samples with and without DCMU poisoning (25 µM final concentration). D. Relative signal intensity for start-point samples with and without DCMU poisoning.

(Fig. 2A).

Looking at the long-term value, φ_0 and Ψ_0 stabilize at values that are very close to the ones obtained with the same strain under prolonged photosynthetic cultures in similar conditions in the past in our laboratory (0.78 ± 0.02 and 0.36 ± 0.03, respectively). (Fig. 2A).

3.3. Step three: Restoring light-harvesting capabilities

While PSII recovery is on its way, the cells also upregulate their light absorption cross-section (Fig. 2 A). This part of the acclimation process unfolds between 8 and 38.6 ± 3.2 h after light reintroduction. The overall trend is not a first-order dynamic *per se*, as it features a rapid rise followed by a slower dynamic. Nevertheless, a characteristic time of 31.8 ± 1.6 h can be extracted.

3.4. Step four: Proliferating

After 24 h, flow cytometry readings indicates (Fig. 2 B) that cells divide as two populations (small and large cells) can be observed. These divisions are preceded by morphological modifications, with cells getting progressively larger from 8 to 20 h. Flow cytometry also informs about cell viability during the trophic conversion process. Over the experiment, cell viability remained above 98 % (See Supplementary Materials).

3.5. Step five: Faring

From day 3 onward, all the monitored indicators stabilize, and cells proliferate at a steady rate. After 7 days, the experiments are stopped, and cells are harvested for end-point analyses. As the sample is large, it allows going further in terms of analytics and exploring the two classical goals of a trophic conversion: pigments and protein contents. After 7 days of exposure to 60 µmolPhoton/m^2/s, the cells contain 27.32 ± 1.50 mg/g of chlorophyll *a*, 8.41 ± 0.56 mg/g of chlorophyll *b*, and 6.53 ± 0.25 mg/g of total carotenoids. This profile is to be compared to the initial one, which contained 3.87 +/- 0.23, 3.14 ± 0.16, and 2.10 ± 0.12 mg/g of chlorophyll *a*, *b*, and total carotenoid, respectively. On the protein side, the cell went from 14.60 ± 0.00 g/100 g to 42.63 ± 1.53 g/100 g over the duration of the experiments. Overall, in three days, the trophic conversion process led to a 3 to 10-fold improvement of the

biomass quality, depending on the indicator considered.

3.6. Light intensity modulates end-points, but not the overall dynamic

Exploring further the trophic conversion mechanism, the experiments were repeated under three different light intensities. The range of illumination was extended from 30 to 600 μmol photons/m^2/s to capture the breadth of conditions encountered in both laboratory and industrial outdoor systems. This approach aims to unravel how light intensity shapes the photosynthetic reactivation process. 30 μmolPhoton/m^2/s (only twice the intensity required for photosynthesis to surpass maintenance (Pozzobon, 2020) was used to test a potential energetic limitation of the trophic conversion process. 300 μmolPhoton/m^2/s was conducted to examine how microalgae phenotype evolves when placed under a photosaturating light (See Supplementary Materials). Lastly, 600 μmolPhoton/m^2/s was retained to explore trophic conversion under a light intensity considered as growth-hindering for this strain (Calculation of new nitrogen-to-protein conversion factors, 2004).

Overall, all the runs exhibited a response consistent with the previously described pattern: an initial lag phase followed by a first-order response. φ_0 value started around 0.1 to reach final values between 0.6, under high light conditions, to 0.8, under moderate and low light conditions (See Supplementary Materials). Ψ_0 also shows a common starting point (around 0.03), condition-dependent end-points (0.25 to 0.4), and a first-order dynamic (See Supplementary Materials). Finally, the same goes for the cell absorption cross-section (Fig. 4 A).

Diving further into detail, these time series can be compared along

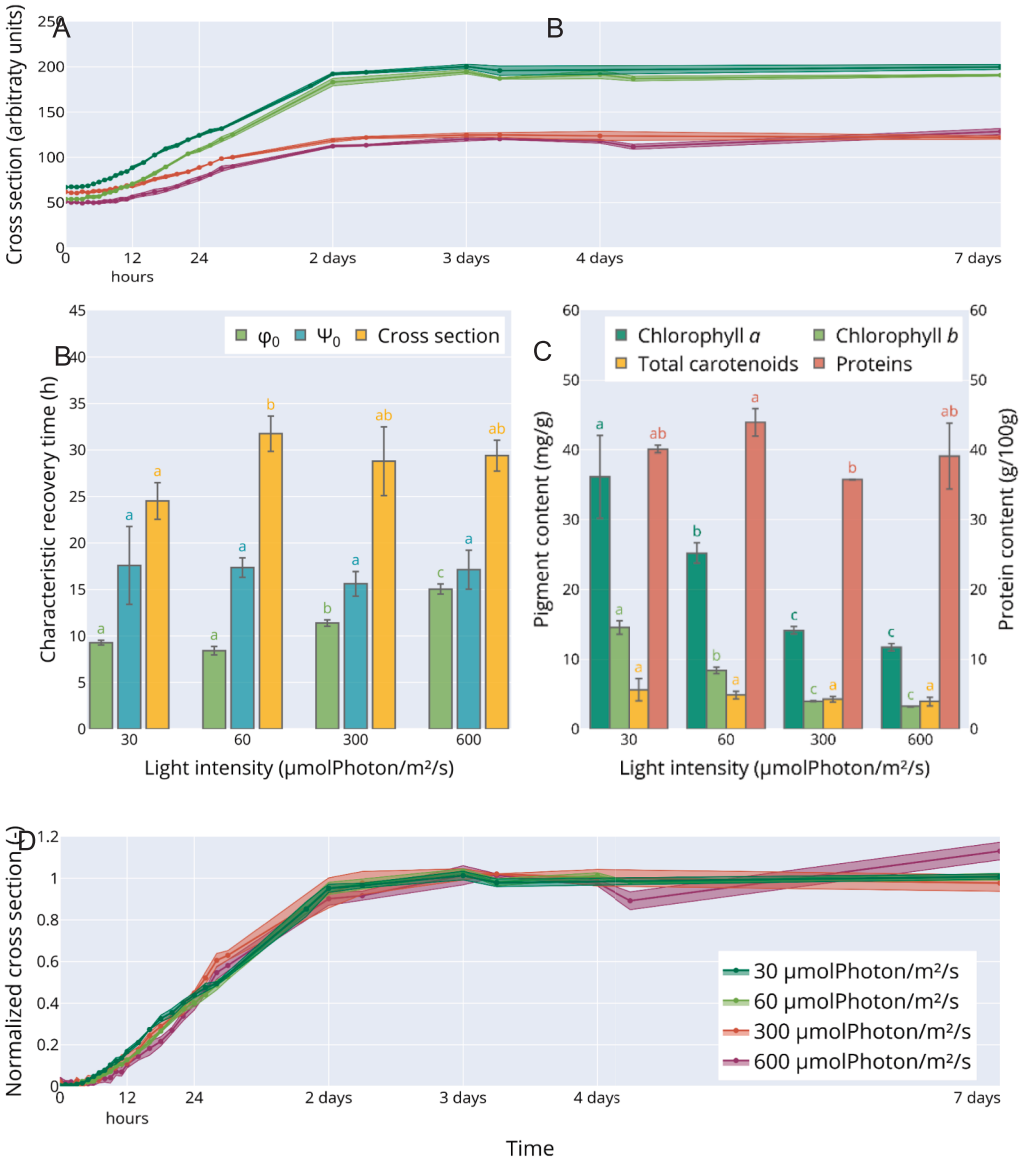

Fig. 4. Trophic conversion process indicators of *Chlorella vulgaris* under 30, 60, 300, and 600 μmolPhoton/m^2/s (inoculum age: 11 days). A. Absolute values of the cross-section over time. B. Characteristic times of φ_0 and Ψ_0 recoveries as well as pigment expression. Data were obtained by fitting experimental data with a first-order response model (one model, hence one time per run). Presented as average and standard deviation (n = 3). Letters – Statistical significance (ANOVA, post-hoc Honestly Significant Difference with Bonferroni correction, $p < 0.05$). C. End-point biomass composition. Pigments were obtained by methanol extraction and spectrophotometric quantification. Protein contents were obtained by total nitrogen quantification and the use of a conversion factor (4.57) specific to a *Chlorella* species (Sullivan and Feinn, 2012). Letters – Statistical significance (ANOVA, post-hoc Honestly Significant Difference with Bonferroni correction, $p < 0.05$). D. Normalized cross-section over time (normalization by overall minima and maxima, for each run taken individually). Solid line – mean of the three replicates. Shaded area – standard deviation (n = 3). Points – Measurements.

two dimensions: their characteristic times and their final values. Fig. 4 A displays the results focusing on trophic conversion characteristic times. The light energy trapping process (φ_0) recovery exhibits a light-intensity dependent time scale ($p = 0.000$). In the case of 30 and 60 μmolPhoton/m^2/s, the repair process unfolds in about 8.9 h. This duration rises to 11.3 h under 300 μmolPhoton/m^2/s and 15.0 h under 600 μmolPhoton/m^2/s. On the contrary, the evolution of its electron-claiming counterpart (Ψ_0) appears light-insensitive, with a characteristic time of 16.7 ± 2.2 h shared among the tested condition ($p = 0.630$). Finally, the pigment expression dynamic (Fig. 4 A&D) shows a dynamic modulated by light intensity ($p = 0.045$). This marginal difference would point toward a lower intensity, allowing for faster acclimation. Still, while a steeper start might be detected on full-scale signals (Fig. 4 A), it is much harder to spot on a normalized graph (Fig. 4 D), making a solid claim of a marked difference look bold.

Fig. 4 C focuses on the final pigment and proteins profiles. Chlorophyll *a* and *b* are strongly modulated by the illumination ($p = 0.000$, for the two pigments) with final values ranging from 36.14 ± 4.83 and 14.53 ± 0.77 mg/g under 30 μmolPhoton/m^2/s down to 11.71 ± 0.46 and 3.25 ± 0.04 mg/g under 600 μmolPhoton/m^2/s. Jointly, the chlorophyll *b*/*a* ratio and the carotenoids/chlorophylls ratio evolve substantially, divided by 1.5 and multiplied by 2.4, respectively (See Supplementary Materials). On the contrary, *Chlorella vulgaris* final protein content is only marginally modulated by the illumination under which the trophic conversion happened ($p = 0.043$), with an averaged value of 39.7 ± 3.8 g/100 g.

3.7. The cells' initial condition does not influence their acclimation dynamics

Another variable that could influence the trophic conversion process is the physiological state of the inoculum. To investigate a potential effect, an aliquot of a 6-day-old culture was run through the trophic conversion process under 60 μmolPhoton/m^2/s (versus 11 days for the previously).

Shortening the inoculum incubation time had an effect on its pigment and protein contents (max p-value = 0.003) and the PSII status (all p-values = 0.000) (Table 1). Overall, the younger inoculum had higher pigment contents (almost tripled chlorophyll *a* and *b* content) and protein content (+69 %). Despite these initial differences, the cells originating from the two inocula exhibit the same phenotype once the trophic conversion is completed. Only two minor discrepancies can be noted in the total carotenoid content and Ψ_0. However, it is important to analyze their absolute values on top of the statistical significance of their difference (Strasser et al., 2000). Upon examination, it can be concluded that they are too close to call for a meaningful phenotypic deviation.

In terms of acclimation dynamics, the φ_0 and cross-section signals were not influenced by the difference in initial conditions ($p = 0.348$ and 0.224, respectively) (See Supplementary Materials). Only Ψ_0 recovery is altered with a time markedly shorter for the younger inoculum, which features a superior physiological status at the start of the trophic conversion (characteristic time of 11.1 ± 0.6 h, vs 17.4 ± 0.9).

Table 1
Comparison of the microalgae physiological status at the beginning and the end of the trophic conversion process. Regular inoculum has a preparation duration of 11 days. Younger inoculum has a preparation duration of 6 days. All preparation conditions were kept the same between the two tests. The trophic conversion process was led under 60 μmolPhoton/m2/s. Overall viability (not reported in the table) was above 98 % (See Supplementary Materials). In addition to composition indicators, characteristic times for PSII recovery and pigment expression can be found in Extended Data (See Supplementary Materials). Results presented as average and standard deviation (n = 3). Formatting – Statistical significance (Welch's *t*-test, two-sided, bold $p < 0.01$, underlined $p < 0.05$).

Indicator (Unit)	Initial state		Final state	
	Regular inoculum	Younger inoculum	Regular inoculum	Younger inoculum
Chlorophyll *a* (mg/g)	**3.87 ± 0.23**	**11.09 ± 0.60**	27.32 ± 1.50	25.2 ± 1.18
Chlorophyll *b* (mg/g)	**1.25 ± 0.10**	**3.14 ± 0.16**	8.41 ± 0.56	8.4 ± 0.39
Total carotenoids (mg/g	**2.1 ± 0.12**	**3.56 ± 0.22**	6.53 ± 0.25	4.86 ± 0.45
Proteins (g/100 g)	**14.6 ± 0.00**	**24.63 ± 0.00**	42.63 ± 1.53	43.93 ± 1.59
φ_0 (abitrary units)	**0.09 ± 0.00**	**0.45 ± 0.00**	0.75 ± 0	0.76 ± 0.02
Ψ_0 (abitrary units)	**0.02 ± 0.00**	**0.21 ± 0.00**	0.39 ± 0.01	0.37 ± 0.01
Cross Section (abitrary units)	**53.96 ± 0.00**	**115.96 ± 0.00**	191.85 ± 2.61	190.77 ± 1.01

4. Discussion

From a metabolic perspective, in these experiments, the trophic conversion required the cells to shift their energetic metabolism from an exogenous organic carbon source to an endogenous, photosynthesis-based one (Fig. 5). In terms of biochemical reactions, the two pathways can swap at the G3P level of the glycolysis cascade. Indeed, in the case of heterotrophy, the glycolysis cascade that supplies pyruvate to the TCA cycle features G3P as an intermediate. Still, when photosynthesis is relied on, G3P changes status. It goes from an intermediate molecule to the primary output of the Calvin-Benson-Bassham cycle (a.k.a. the dark reactions of photosynthesis). Still, while simple from a conceptual point of view, photosynthesis takeover requires a dormant chloroplast to recover its full functionality. Monitoring this recovery was the goal of these investigations.

Prolonged heterotrophic growth has strongly altered cell physiological state. Cell protein content was around 15 g/100 g, which is far below the commonly reported 40 to 50 g/100 g for phototrophic *Chlorella* cells (Madeira, 2017). Pigment contents were also particularly low, with a total pigment content of 10 mg/g, compared to 40 to 120 mg/g for their photosynthetic counterpart (light intensity dependent). Still, the most impacted part of the phenotype might be PSII functioning. Initial transient PSII fluorescence recordings exhibited high-intensity and almost flat signals, which contrast dramatically with the expected behavior (a multi-step rise followed by a fall [35]). These readings suggest that the process could fail at three levels: light energy channeling to the special pair of chlorophyll *a* (φ_0), the electron recovery by the special pair of chlorophyll *a* (Ψ_0), and the transfer of electron flow to the plastoquinone molecule. By showing no difference with the conventional assays, the tests in the presence of DCMU confirmed that the observed effects were related to the PSII only and not to the pool of plastoquinone. In addition, the lack of an early inflection on the OJIP profiles indicated that the antenna chlorophylls were unable to transfer excitation energy to the reaction center. Collectively, these elements point toward an almost complete disconnection of the PSII antennae from the reaction centers. Still, it is difficult to compare these results with other scholars' work as such initial readings were not reported by other authors, suggesting that their cells might not have acclimated fully to heterotrophy (Levasseur et al., 2023).

The recovery from this prejudicial initial state unfolds in steps. It first starts with a 3 to 4-hour lag phase. It can be hypothesized that this period is dedicated to gene expression and the production of the RNA controlling the biosynthesis of the upcoming proteins. This duration can even represent a means to assess stress severity. Indeed, it is possible to evaluate the minimum delay between a life-threatening environmental change and the phenotypic response involving *de novo* protein synthesis. To do so, simple considerations on gene expression (translocation, preparation, and translation) can be drawn. Taking the *Chlorella* NC64 genome as reference, an average gene length of 4.7 kb can be considered (Ben-Tabou de-Leon, S. & Davidson, E. H., 2009). Then, the translocation rate can be evaluated around 12–18b/s at 25 °C, the mRNA preparation time around 10–30 min, and the translation rate at 3.6

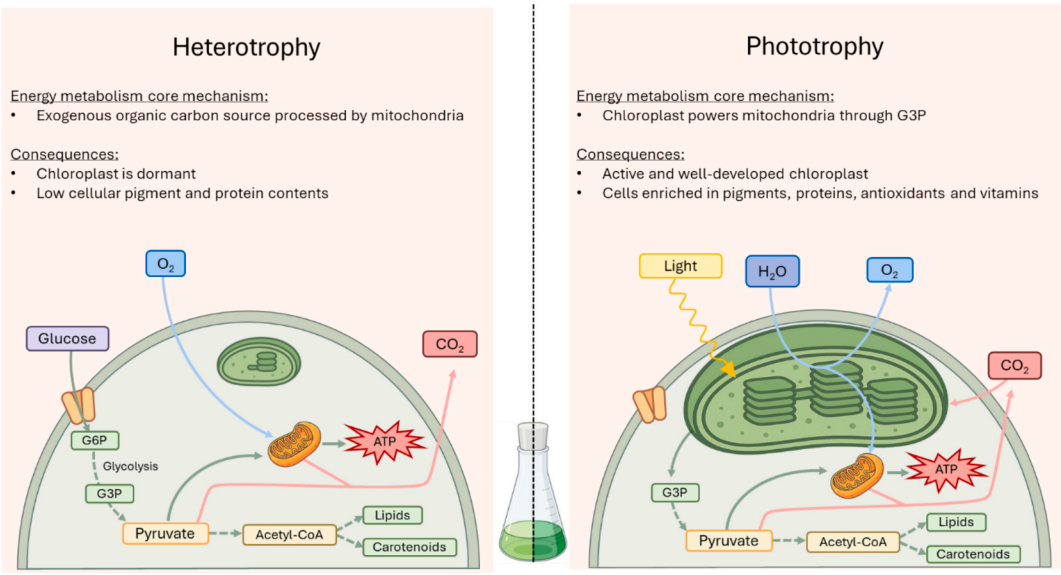

Fig. 5. Schematic representation of simplified metabolic pathways in microalgae under heterotrophic and phototrophic conditions. The main difference lies in the origin of glyceraldehyde-3-phosphate (G3P), a central metabolic intermediate. In heterotrophy, G3P derives from glycolysis of exogenous glucose, whereas in phototrophy, it is produced by the Calvin-Benson-Bassham cycle within the chloroplast, driven by light energy. In both cases, G3P subsequently feeds into the mitochondria for respiration. Green arrows represent metabolic fluxes, red and blue arrows indicate CO_2 and O_2 production or consumption, respectively, and yellow arrows represent light energy.

amino acid/s (at 25 °C) (Lv, 2021). Altogether, these elements yield a theoretical lower limit for this duration between 20 and 45 min. This estimate is consistent with prior observations in *Dunaliella salina*, where acclimation to osmotic stress involves gene transcription within 1 h and protein synthesis within 2 h (Sun et al., 2016). In the case of softer environmental condition shifts, this delay tends to lengthen. For example, after a CO_2 shift, *Chlorella pyrenoidosa* requires up to 2 to 6 h to show observable photosynthetic gene expression (Bonnanfant et al., 2019). Therefore, with a 3 to 4-hour induction time, it can be concluded that the trophic conversion process is not perceived as a major stress by the cells.

Following this gene expression period, the first phenotypically noticeable changes are related to the functioning of the PSII. Light energy channeling to the reaction center is the primary target for PSII repair. It shows a first-order dynamic with a characteristic time varying with incident light (from 9 h under 30 μmolPhoton/m^2/s to 15 h under 600 μmolPhoton/m^2/s). In contrast, electron recovery (Ψ_0) progresses independently of light conditions, requiring approximately 17 h across all the tested light intensities. In the absence of direct ROS measurements, two explanations can be hypothesized for φ_0 recovery dynamic light dependency. Either, newly available light overloads the systems and triggers photodamage (Li, 2020) and slows down the recovery process. Alternatively, the process could be regulated by the cells to avoid capturing too much light that would be mismanaged and lead to photodamage. The second explanation appears to be the right one. Indeed, PSII damages impact electron recovery (Ψ_0) (Geider et al., 1998), incidentally slowing it down, which is not the case here. The argument of a controlled recovery is reinforced by the fact that, overall, the younger inoculum (6 days of incubation) evolves at the same speed as its older counterpart (11 days of incubation), despite a more favorable initial physiological state. Finally, this interpretation also aligns with the earlier conclusion regarding lag phase duration, reinforcing the notion that the trophic conversion constitutes a relative stress.

The second phenotypical change is the increase in the cell pigment content. First of all, its 4 to 8 h lag is in agreement with Babaei et al.'s work (Levasseur et al., 2023). Unfortunately, the authors did not investigate trophic conversion on a time scale large enough to identify a characteristic time. Luckily, other authors monitored *Chlorella* species pigment acclimation over several days (*Chlorella vulgaris, Chlorella ellipsoidea, Chlorella pyrenoidosa* (Fan, 2012); *Chlorella pyrenoidosa* [15]). In their work, they observed that the cells required around 24 h to reach their final pigmentation (12-hour sampling frequency does not allow being more accurate). Taken together, these observations are consistent with other teams' reports and underline the need of high-frequency monitoring when investigating a trophic conversion process.

Finally, end-point analysis confirms that the cells recovered a photosynthetic phenotype. A protein content between 40–50 g/100 g is classically reported for *Chlorella* sp. under phototrophic conditions (Madeira, 2017). Pigment contents are more difficult to compare precisely, as microalgae are known to exhibit different pigment profiles and overall behavior depending on the illumination they are subjected to. Nevertheless, the trend (higher light leading to lower pigment content) and the values are in line with other scholars' reports (MacIntyre et al., 2002; Andersen, 2005).

5. Conclusion

Taking a step back, from a biotechnological perspective, it can be concluded that the end-point of a trophic conversion aligns with classical microalgae knowledge. This opens the way to leverage existing expertise to tailor the final biomass quality. However, strong divergences also exist. The most dire one might be the fact that the acclimation dynamic is only marginally affected by the incident intensity. Indeed, cells repair and synthesize their photosynthetic machinery in a controlled manner. This way, they avoid photodamage, even under high light conditions. These two observations bear significant meaning at the bioprocess level: a low-light process is advisable as it will deliver high-quality microalgae, and limit the process's ecological impact if artificial light is resorted to. Still, as sunlight intensity naturally fluctuates, and the cell be subjected to mutual shading, achieving the required level of control to follow these intrinsic metabolic guidelines is challenging.

CRediT authorship contribution statement

Wendie Levasseur: Writing – review & editing, Visualization,

Validation, Methodology, Investigation, Formal analysis, Conceptualization. **Victor Pozzobon:** Writing – original draft, Visualization, Validation, Software, Methodology, Investigation, Funding acquisition, Formal analysis, Data curation, Conceptualization.

Declaration of competing interest

The authors declare that they have no known competing financial interests or personal relationships that could have appeared to influence the work reported in this paper.

Acknowledgments

This project was funded by the French government as part of the France 2030 initiative. Communauté urbaine du Grand Reims, Département de la Marne, Région Grand Est and European Union (FEDER Champagne-Ardenne 2014-2020, FEDER Grand Est 2021-2027) are acknowledged for their financial support to the Chair of Biotechnology of CentraleSupélec and the Centre Européen de Biotechnologie et de Bioéconomie (CEBB).

Appendix A. Supplementary Material

Supplementary data to this article can be found online at https://doi.org/10.1016/j.biortech.2025.133262.

Data availability

Data will be made available on request.

References

Andersen, R.A., 2005. *Algal Culturing Techniques*. Academic Press.
Babaei, A., et al., 2020. Photobiochemical changes in Chlorella g120 culture during trophic conversion (metabolic pathway shift) from heterotrophic to phototrophic growth regime. J. Appl. Phycol. 32, 2807–2818.
Barron, J. T. A General and Adaptive Robust Loss Function. in 4331–4339 (2019).
Barros, A., et al., 2019. Heterotrophy as a tool to overcome the long and costly autotrophic scale-up process for large scale production of microalgae. Sci. Rep. 9, 13935.
Behrenfeld, M.J., et al., 2001. Biospheric primary production during an ENSO transition. Science 291, 2594–2597.
Ben-Tabou de-Leon, S., Davidson, E.H., 2009. Modeling the dynamics of transcriptional gene regulatory networks for animal development. Dev. Biol. 325, 317–328.
Blanc, G., et al., 2010. The Chlorella variabilis NC64A genome reveals adaptation to photosymbiosis, coevolution with viruses, and cryptic sex. Plant Cell 22, 2943–2955.
Bonnanfant, M., Jesus, B., Pruvost, J., Mouget, J.-L., Campbell, D.A., 2019. Photosynthetic electron transport transients in *Chlorella vulgaris* under fluctuating light. Algal Res. 44, 101713.
Brown, N., Shilton, A., 2014. Luxury uptake of phosphorus by microalgae in waste stabilisation ponds: current understanding and future direction. Rev. Environ. Sci. Biotechnol. 13, 321–328.
Lourenço, S. O., Barbarino, Elisabete, Lavín, Paris L, Lanfer Marquez, Ursula M., and Aidar, E. Distribution of intracellular nitrogen in marine microalgae: Calculation of new nitrogen-to-protein conversion factors. *Eur. J. Phycol.* **39**, 17–32 (2004).
Camarena-Bernard, C., Pozzobon, V., 2024. Evolving perspectives on lutein production from microalgae – a focus on productivity and heterotrophic culture. Biotechnol. Adv. 73, 108375.
Chen, J.-H., et al., 2022. A novel and effective two-stage cultivation strategy for enhanced lutein production with *Chlorella sorokiniana*. Biochem. Eng. J. 188, 108688.
de Mooij, T., Schediwy, K., Wijffels, R.H., Janssen, M., 2016. Modeling the competition between antenna size mutant and wild type microalgae in outdoor mass culture. J. Biotechnol. 240, 1–13.
Degen, J., Uebele, A., Retze, A., Schmid-Staiger, U., Trösch, W., 2001. A novel airlift photobioreactor with baffles for improved light utilization through the flashing light effect. J. Biotechnol. 92, 89–94.
Fan, J., et al., 2012. Sequential heterotrophy–dilution–photoinduction cultivation for efficient microalgal biomass and lipid production. Bioresour. Technol. 112, 206–211.
Geider, R.J., MacIntyre, H.L., Kana, T.M., 1998. A dynamic regulatory model of phytoplanktonic acclimation to light, nutrients, and temperature. Limnol. Oceanogr. 43, 679–694.
Gladue, R.M., Maxey, J.E., 1994. Microalgal feeds for aquaculture. J. Appl. Phycol. 6, 131–141.
Ho, S.-H., et al., 2013. Characterization and optimization of carbohydrate production from an indigenous microalga *Chlorella vulgaris* FSP-E. Bioresour. Technol. 135, 157–165.
Hutchins, D.A., Fu, F., 2017. Microorganisms and ocean global change. Nat. Microbiol. 2, 17058.
Kim, U., et al., 2020. Two-stage cultivation strategy for the improvement of pigment productivity from high-density heterotrophic algal cultures. Bioresour. Technol. 302, 122840.
Levasseur, W., Perré, P., Pozzobon, V., 2023. *Chlorella vulgaris* acclimated cultivation under flashing light: an in-depth investigation under iso-actinic conditions. Algal Res. 70, 102976.
Levine, N.M., Leles, S.G., 2021. Marine plankton metabolisms revealed. Nat. Microbiol. 6, 147–148.
Li, S., et al., 2020. Influence of polystyrene microplastics on the growth, photosynthetic efficiency and aggregation of freshwater microalgae *Chlamydomonas reinhardtii*. Sci. Total Environ. 714, 136767.
Lichtenthaler, H.K., Buschmann, C., 2001. Chlorophylls and carotenoids: measurement and characterization by UV-VIS spectroscopy. Curr. Protoc. Food Anal. Chem. 1. F4.3.1-F4.3.8.
Lv, H., et al., 2021. Comparative transcriptome analysis of short-term responses to salt and glycerol hyperosmotic stress in the green alga *Dunaliella salina*. Algal Res. 53, 102147.
MacIntyre, H.L., Kana, T.M., Anning, T., Geider, R.J., 2002. Photoacclimation of photosynthesis irradiance response curves and photosynthetic pigments in microalgae and cyanobacteria. J. Phycol. 38, 17–38.
Madeira, M.S., et al., 2017. Microalgae as feed ingredients for livestock production and meat quality: a review. Livest. Sci. 205, 111–121.
Masojídek, J., et al., 2021. Changes in photosynthesis, growth and biomass composition in outdoor *Chlorella* g120 culture during the metabolic shift from heterotrophic to phototrophic cultivation regime. Algal Res. 56, 102303.
Moheimani, N. R., Borowitzka, M. A., Isdepsky, A. Sing, S. F. Standard Methods for Measuring Growth of Algae and Their Composition. in *Algae for Biofuels and Energy* (eds. Borowitzka, M. A. & Moheimani, N. R.) 265–284 (Springer Netherlands, Dordrecht, 2013). doi:10.1007/978-94-007-5479-9_16.
Ogbonna, J.C., Masui, H., Tanaka, H., 1997. Sequential heterotrophic/autotrophic cultivation – an efficient method of producing Chlorella biomass for health food and animal feed. J. Appl. Phycol. 9, 359–366.
Oliver, A., Camarena-Bernard, C., Lagirarde, J., Pozzobon, V., 2023. Assessment of photosynthetic carbon capture versus carbon footprint of an industrial microalgal process. Appl. Sci. 13, 5193.
Porra, R.J., 1990. A simple method for extracting chlorophylls from the recalcitrant alga, *Nannochloris atomus*, without formation of spectroscopically-different magnesium-rhodochlorin derivatives. Biochim. Biophys. Acta BBA - Bioenerg. 1019, 137–141.
Posadas, E., del Morales, M., Gomez, C., Acién, F.G., Muñoz, R., 2015. Influence of pH and CO2 source on the performance of microalgae-based secondary domestic wastewater treatment in outdoors pilot raceways. Chem. Eng. J. 265, 239–248.
Pozzobon, V., et al., 2020. Machine learning processing of microalgae flow cytometry readings: illustrated with Chlorella vulgaris viability assays. J. Appl. Phycol. 32, 2967–2976.
Pulz, O., 2001. Photobioreactors: production systems for phototrophic microorganisms. Appl. Microbiol. Biotechnol. 57, 287–293.
Qiang, H., Zarmi, Y., Richmond, A., 1998. Combined effects of light intensity, light-path and culture density on output rate of Spirulina platensis (Cyanobacteria). Eur. J. Phycol. 33, 165–171.
Ronzon, T., Tamosiunas, S. & M'barek, R. Jobs and growth in the bioeconomy. *JRC Publications Repository* https://publications.jrc.ec.europa.eu/repository/handle/JRC128361 (2022) doi:10.2760/323093.
Ruiz, J., et al., 2016. Towards industrial products from microalgae. Energy Environ. Sci. 9, 3036–3043.
Seabold, S., Perktold, J., 2010. Statsmodels: Econometric and Statistical Modeling with Python. in 92–96 (Austin, Texas). doi:10.25080/Majora-92bf1922-011.
Shibata, K., 1959. Spectrophotometry of translucent biological materials—opal glass transmission method. In: Methods of Biochemical Analysis. John Wiley & Sons Ltd, pp. 77–109. https://doi.org/10.1002/9780470110232.ch3.
Strasser, R., Srivastava, A. & Tsimilli-Michael, M. The fluorescence transient as a tool to characterize and screen photosynthetic samples. in (2000).
Sullivan, G.M., Feinn, R., 2012. Using effect size—or why the P value is not enough. J. Grad. Med. Educ. 4, 279–282.
Sun, X., Shen, J., Bai, F., Xu, N., 2016. Transcriptome profiling of the microalga *Chlorella pyrenoidosa* in response to different carbon dioxide concentrations. Mar. Genomics 29, 81–87.
Wan, M., et al., 2015. Sequential heterotrophy–dilution–photoinduction cultivation of haematococcus pluvialis for efficient production of astaxanthin. Bioresour. Technol. 198, 557–563.
Wang, J., Zhou, W., Yang, H., Wang, F., Ruan, R., 2015. Trophic mode conversion and nitrogen deprivation of microalgae for high ammonium removal from synthetic wastewater. Bioresour. Technol. 196, 668–676.
Wellburn, A.R., 1994. The spectral determination of chlorophylls *a* and *b*, as well as total carotenoids, using various solvents with spectrophotometers of different resolution. J. Plant Physiol. 144, 307–313.
Xie, T., Xia, Y., Zeng, Y., Li, X., Zhang, Y., 2017. Nitrate concentration-shift cultivation to enhance protein content of heterotrophic microalga *Chlorella vulgaris*: Over-compensation strategy. Bioresour. Technol. 233, 247–255.

Zhang, Z., et al., 2025. Two-stage trophic strategy coupled with fed-batch operation for simultaneous enhancement of cell growth and lutein synthesis in *Chlorella sorokiniana*. Biochem. Eng. J. 215, 109632.
Zheng, Y., Chi, Z., Lucker, B., Chen, S., 2012. Two-stage heterotrophic and phototrophic culture strategy for algal biomass and lipid production. Bioresour. Technol. 103, 484–488.
Zhou, W., et al., 2012. A hetero-photoautotrophic two-stage cultivation process to improve wastewater nutrient removal and enhance algal lipid accumulation. Bioresour. Technol. 110, 448–455.